

Rapid Communications

The Rapid Communications section is intended for the accelerated publication of important new results. Manuscripts submitted to this section are given priority in handling in the editorial office and in production. A Rapid Communication may be no longer than 3½ printed pages and must be accompanied by an abstract. Page proofs are sent to authors, but, because of the rapid publication schedule, publication is not delayed for receipt of corrections unless requested by the author.

New model of the temperature dependence of the 1.4-eV emission band of amorphous silicon

F. Boulitrop, D. J. Dunstan,* and A. Chenevas-Paule

Commissariat à l'Energie Atomique, Centre d'Etudes Nucléaires de Grenoble, Laboratoire d'Electronique et de Technologie de l'Informatique/Composants Electroniques, Department de Recherche Fondamentale/Resonance Magnetique, F-38041, Grenoble Cédex, France

(Received 23 March 1982)

Time-resolved measurements of the quenching of the long decay components of the 1.4-eV luminescence of *a*-Si:H show that the mechanisms of thermally induced lifetime redistribution and thermal quenching are distinct. We identify the mechanisms as, respectively, electron and hole diffusion. This model implies distant-pair kinetics for the photoluminescence. Comparison of the activation energies found from the photoluminescence with those of the mobility suggest that the mobility is due, not to thermal excitation to a mobility edge, but to percolation in potential fluctuations of a length of some 100 Å.

The 1.4-eV photoluminescence (PL) of *a*-Si:H is quenched thermally above about 100 K with an activation energy in the range 120–250 meV.¹⁻⁴ Although at sufficiently high temperature the quenching curve can be described by an expression of the form

$$I(T) = \frac{I_0 \tau_r^{-1}}{\tau_r^{-1} + \tau_{nr}^{-1}(T)}, \quad (1)$$

with the nonradiative recombination rate τ_{nr}^{-1} given by

$$\tau_{nr}^{-1} = u [\exp(E_a/kT) - 1]^{-1}. \quad (2)$$

For values of $I/I_0 \sim 1$ the curve deviates significantly from Eq. (1); the elbow of the experimental curve being much smoother (see Fig. 1 curves a). Also, at low temperature, the intensity is often observed to fall from its maximum value in the region of 50–70 K.⁵

The behavior of the PL in the region of the elbow has been studied using plots of $\log_{10}(I_0/I - 1)$ against T^{-1} or against T^2 . These plots are sensitive to the choice of I_0 ; if suitably chosen, the plot against T^{-1} shows evidence of two activation energies of quenching: $E_a \sim 70$ meV in the region $70 < T < 100$ K and $E_a \sim 200$ meV above about 120 K.² On the other hand, the plot against T can give a straight line² which Street⁶ has discussed in terms of the model of Higashi and Kastner⁷ of a distribution of values of the activation energy. However, the PL has a very

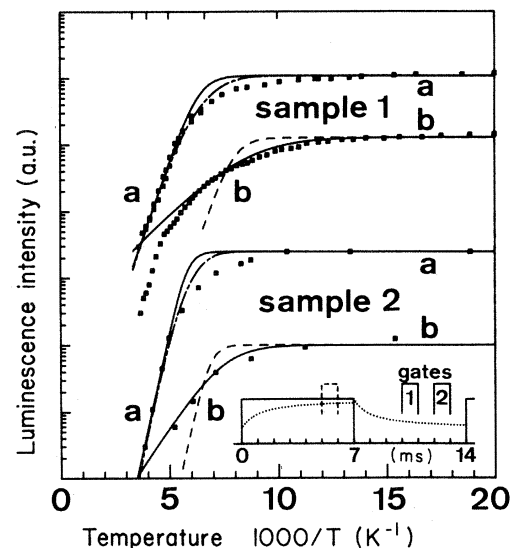


FIG. 1. For two samples of *sp a*-Si:H we show the thermal quenching curves of (a) the total PL intensity and of (b) the long-lived components, measured according to the timing diagram inset. The solid curves (a) are fits using Eq. (1); the chain-dotted curves (a) are for a distribution of τ_r , Eq. (3). The broken curves are the expected fits to the data for the long-lived components, using parameter values obtained from the total PL; the solid curves (b) are fits using Eq. (1) with different parameter values. All parameters used are listed in Table I.

TABLE I. Parameters used in Eqs. (1) and (3) to generate the curves of Fig. 1.

	E_a (meV)	u (s^{-1})	τ_r (s)	I_0 (a.u.)
Sample 1				
Solid curve a	180	10^{10}	10^4	1100
Chain-dotted curve a	200	$10^{11.2}$	$10^4 \pm 1$	1100
Solid curve b	60	$10^{5.2}$	$10^{2.5}$	130
Broken curve b	180	10^{10}	$10^{2.5}$	130
Sample 2				
Solid curve a	280	$10^{12.5}$	10^4	2.5
Chain-dotted curve a	300	$10^{13.8}$	$10^4 \pm 1$	2.5
Solid curve b	95	$10^{6.2}$	$10^{2.5}$	0.1
Broken curve b	280	$10^{12.5}$	$10^{2.5}$	0.1

wide distribution of radiative lifetimes $P(\tau_r)$, extending from 10 ns to at least 10 ms,⁴ and we have pointed out elsewhere⁸ that this will have a significant effect on the form of the quenching curve. With a $P(\tau_r)$, Eq. (1) becomes

$$I(T) = I_0 \int_0^\infty P(\tau_r) \frac{\tau_r^{-1}}{\tau_r^{-1} + \tau_{nr}^{-1}(T)} d\tau_r. \quad (3)$$

From the experimental data,^{4,9} $P(\tau_r)$ may be represented approximately by a Gaussian in $\log(\tau_r)$ of one decade half-width at half height. The peak position varies with the temperature and excitation power, but may be taken here as 0.3 ms. Using this distribution, we have integrated Eq. (3) numerically and, with the parameters given in Table I we obtain the chain-dotted curves (a) of Fig. 1, which are a much closer fit to the experimental data than are the solid curves (a) from Eq. (1). It may be, then, that the lifetime distribution accounts for much of the deviation of the data from Eq. (1).

In order to study the remainder of the discrepancy, we have made time-resolved measurements of the quenching curve. By selecting only a small part of the lifetime distribution, we expect to obtain a quenching curve closer to Eq. (1) and whose difference from Eq. (1) may properly be discussed in terms of, for example, a distribution of activation energies.

The lifetime distribution is itself temperature dependent; this is supposed to be due to the same mechanism as the quenching.⁶ Since $P(\tau_r)$ shifts to shorter times at high temperature,⁶ we have measured the longer components of the decay ($\tau \sim 4$ ms) in order to avoid the complications that would ensue at short τ as the shift in the distribution brought different components past the detection gate.

The experiment was carried out using a dual channel boxcar in subtraction mode, in order to avoid the

problems that can arise in conventional time-resolved spectroscopy when the repetition rate of the excitation pulses is faster than the longest lifetimes in the emission.⁹ Sputtered *a*-Si:H samples with a dark EPR spin density $\sim 5 \times 10^{15} \text{ cm}^{-3}$ and which showed efficient PL were used, and the PL spectra were corrected for the response of the detection system. Spectra were recorded at different temperatures, using the two gates of the boxcar set at 3 and 5 ms after the cutoff of the 70-Hz square-wave excitation; the difference between the two channels gives approximately the components of the PL with $\tau \sim 4$ ms. The total PL was measured using a single gate set near the end of the excitation. A timing diagram is inset in Fig. 1. We also checked the effect of dark EPR spin density on the quenching curve in a single sample, by driving off some of the hydrogen in anneals at various temperatures. In agreement with the results of Street,⁶ the activation energy was decreased by spin densities of 10^{17} cm^{-3} upwards (Fig. 2). The quenching curves for low spin density are shown in Fig. 1. The total PL data are the points marked a; the results for the long-lived components of the PL are the points marked b. The elbow of the quenching curve has become even more rounded than that of the total PL.

This result is quite unexpected. While in eliminating the smoothing effect of the lifetime distribution we expect to obtain something like the broken curves (b), calculated from Eq. (1) with the parameters u and E_a of the total PL and $\tau_r = 4$ ms (Table I), in fact the results are much better described by Eq. (1) (up to ~ 200 K) with entirely different parameters (Table I). In particular, the activation energy is less than half the value for the total PL.

It is clear that the quenching of the long-lived components corresponds partly to the redistribution of lifetimes, rather than to nonradiative recombination. Nevertheless, according to the geminate model of the PL mechanism (reviewed by Street⁶) the redistribution of lifetimes is due to carrier diffusion just as is thermal quenching. The only difference is that at low

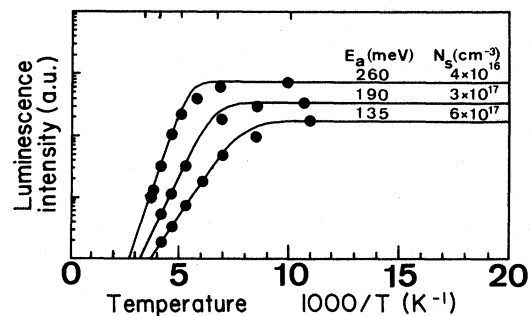


FIG. 2. Quenching curves for a single sample of *sp a*-Si:H for the values of the EPR spin density (marked). Note the effect of spin densities as low as 10^{17} cm^{-3} .

temperature the Onsager radius is greater than the pair separations while at high temperature it is less. In either case diffusion leads to a loss of long-lived components, and the two phenomena are expected to have the same activation energy—that for diffusion of the shallower carrier. Since we find widely different values of the activation energies of the two processes, we have clear evidence that there are two separate mechanisms. Comparing the values of the activation energies with the activation energies of mobility of the carriers (Tiedje *et al.*¹⁰ and references therein), about 100 meV for the electron and 300 meV for the hole, we suggest that the mechanism of the lifetime redistribution is diffusion of the electrons, and that the quenching is due to diffusion of the holes. In this model, nonradiative recombination can only occur when both carriers can diffuse, at temperatures ≥ 100 K (apart, of course, from the temperature-independent nonradiative recombination attributed to tunneling to the defects⁴); at temperatures where only the electrons can diffuse ($50 \leq T \leq 100$ K) the carrier spatial distribution is randomized but nonradiative recombination does not occur. At low temperatures ≤ 50 K both carriers remain trapped—either at random spatially, if the distance between pairs is less than the average separation of a pair (the distant pair model), or according to the geminate model at sufficiently low pair density.

According to the model presented here, above about 50 K, the kinetics of the recombination should be distant pair at all excitation powers, since the diffusion of the electrons randomizes the pairs. This prediction is in contradiction with the results of Street and co-workers, who deduce geminate recombination below a pair density $\sim 10^{18} \text{ cm}^{-3}$,⁶ but it is in agreement with the recent direct measurements of the lifetime distribution made by observing the frequency response of the emission,⁹ which show distant-pair kinetics even at 2 K to the lowest measurable excitation powers ($\sim 2 \cdot 10^{17} \text{ cm}^{-3} \text{ s}^{-1}$), and is also in agreement with the kinetics of the LESR signal.¹¹

It is significant that although we identify the activation energies E_a^Q with E_a^h and E_a^D with E_a^e , the mobility activation energies are in fact greater than the values of E_a^Q and E_a^D reported here. We attribute this difference to a difference between the mobility over macroscopic distances and over distances of the order of 100 Å. Only the latter are relevant to the PL. In support of this suggestion, we note that the activation energy of quenching depends on the density of non-radiative centers (as measured by the dark EPR signal). According to the data of Street⁶ and our own measurements (Fig. 2), the value of E_a^Q is considerably reduced by spin densities above about 10^{17} cm^{-3} , corresponding to diffusion distances ≥ 100 Å. This cannot be understood in terms of diffusion by thermal activation to a mobility edge, when only the pre-factor u should vary with the distance, but is readily explained by a percolation model of transport. Macroscopic transport is dominated by the highest potential barriers along the percolation path; over short distances a carrier is unlikely to encounter the highest potentials and so can diffuse with a lower activation energy. Since this reduction of E_a^Q is already significant for distances of about 100 Å, we deduce that the transport is controlled by potential fluctuations of about this order of length.

In summary, we find that the thermal quenching of the long-lived components of the 1.4-eV PL in α -Si:H is quite different from that of this band as a whole. We deduce that the mechanisms of lifetime redistribution and of thermal quenching are different, and we identify them with the diffusion of, respectively, electrons and holes. This interpretation is consistent with a distant-pair model of the PL kinetics. The activation energies found in these processes are, however, less than those observed in macroscopic transport measurements. Because, also, the activation energy of quenching decreases further with defect densities 10^{17} cm^{-3} , we conclude that carrier mobility is determined by percolation in potential fluctuations with a characteristic length of about 100 Å.

*Present address: Angewandte Physik, Johannes Kepler Universität, 4040 Linz, Austria.

¹D. Engemann and R. Fischer, Phys. Status Solidi (b) **79**, 195 (1977).

²R. W. Collins, M. A. Paesler, and W. Paul, Solid State Commun. **34**, 833 (1980).

³I. G. Austin, T. S. Nashashibi, T. M. Searle, P. G. LeComber, and W. E. Spear, J. Non-Cryst. Solids **32**, 373 (1979).

⁴C. Tsang and R. A. Street, Phys. Rev. B **19**, 3027 (1978).

⁵R. A. Street, Phys. Rev. B **23**, 861 (1981).

⁶R. A. Street, Adv. Phys. **30**, 593 (1981).

⁷G. S. Higashi and M. Kastner, J. Phys. C **12**, L281 (1979).

⁸D. J. Dunstan and F. Boulitrop, Solid State Commun. **39**, 1005 (1981).

⁹D. J. Dunstan, S. Depinna, and B. C. Cavenett, J. Phys. C (in press).

¹⁰T. Tiedje, A. Rose, and J. M. Cebulka, in *Tetrahedrally Bonded Amorphous Semiconductors—1981*, edited by R. A. Street, D. K. Biegelsen, and J. C. Knights, AIP Conf. Proc. No. 73 (AIP, New York, 1981), p. 197.

¹¹F. Boulitrop and D. J. Dunstan (unpublished).